Earth and Planetary Science Letters, 34 (1977) 209–224

[5]

DISTRIBUTION OF THE PRE-SOLAR COMPONENT IN ALLENDE AND OTHER CARBONACEOUS CHONDRITES

ROBERT N. CLAYTON [1], NAOKI ONUMA [2], LAWRENCE GROSSMAN [3] and TOSHIKO K. MAYEDA

Enrico Fermi Institute, University of Chicago, Chicago, Ill. 60637 (USA)

Received August 5, 1976
Revised version received November 26, 1976

Excess ^{16}O, relative to terrestrial abundances, has been found in all samples of C2, C3 and C4 carbonaceous chondrites which have been analyzed, amounting to nine meteorites thus far. Whole-rocks and mineral separates from all the C3 and C4 meteorites fall on a single mixing line consistent with admixture of 1–5% of excess ^{16}O. The anhydrous silicates of C2 meteorites fall on the same line, but the hydrous silicate matrix of C2's define a mass-fractionation trend parallel to the terrestrial trend, but displaced towards higher ^{16}O. All meteorites analyzed are isotopically heterogeneous on a sub-millimeter scale. Detailed analyses of separated phases of several Allende Ca-Al-rich inclusions reveal a consistent pattern of large ^{16}O enrichments in spinel, pyroxene and sometimes olivine, and small ^{16}O enrichments in melilite, feldspathoids and grossular. The heterogeneous distribution of the ^{16}O excesses, together with their enhancement in minerals believed to be early solar nebular condensates, implies the existence of pre-solar "carriers" of the isotopic anomaly, probably grains or molecules with oxygen which was nearly pure ^{16}O. These carriers have not been unequivocally indentified, but pre-solar grains of corundum or spinel, and pre-solar molecules of SiO are possibilities. The isotopic anomalies may also have been disturbed by diffusion-controlled processes of exchange between early condensates and their surroundings, either in the nebula, or later in the parent body. No direct correlation has yet been observed between the oxygen isotope anomalies and recently observed isotope anomalies in neon, magnesium and xenon.

1. Introduction

The carbonaceous chondrites contain oxygen with "anomalous" isotopic abundance patterns which cannot be attributed to the usual processes of mass-dependent isotopic fractionation [1]. In meteorites of type C3, the anomaly corresponds to an excess of ^{16}O amounting to about 1% of the total oxygen of the meteorite. The ^{16}O excess is distributed very heterogeneously within each meteorite [2]. It has been suggested that these isotopic anomalies result from the incorporation into the meteorites of pre-solar dust grains highly enriched in ^{16}O, having had a separate nucleosynthetic history from the bulk of solar system matter [1,2]. The principal aim of this research was to investigate the variations of the ^{16}O-rich component within individual meteorites in an attempt to characterize the carrier of the ^{16}O tracer chemically and mineralogically.

The samples chosen for study were carbonaceous chondrites of types C2, C3 and C4: Murchison and Murray (C2), Allende, Grosnaja, Ornans, Vigarano and Warrenton (all C3), Coolidge and Karoonda (C4). The greatest number of samples came from Allende, in which the relatively abundant large inclusions afforded an opportunity to study the spatial distribution of isotopic abundances on a sub-millimeter scale.

2. Analytical techniques

Mineral separates and concentrates were prepared by a combination of hand-picking, magnetic and heavy-liquid techniques. In the cases of Murchison, Murray,

[1] Also Departments of Chemistry and Geophysical Sciences.
[2] Present address: Department of Chemistry, University of Tsukuba, Sakura-Mura, Ibaragi-Ken, Japan.
[3] Also Department of Geophysical Sciences.

Grosnaja, Ornans, Vigarano, Warrenton, and Karoonda, aside from a few hand-picked samples, separations were carried out on ground-up pieces of the whole meteorite. The various density fractions then consist mostly of different proportions of olivine and pyroxene, and different Fe/Mg ratios in these minerals. Plagioclase and magnetite were also separated from Karoonda. Mineral identifications were based primarily on X-ray powder patterns. In the case of Allende, all of the separations were performed on individual inclusions excavated from sawed surfaces. Some of these same inclusions have been analyzed for major elements by electron microprobe [3] and for trace elements by isotopic dilution and neutron activation [4]. Some have had magnesium and strontium isotope analyses [5,6].

Oxygen was extracted for mass spectroscopy by the bromine pentafluoride procedure [7], and was analyzed as O_2 in most cases to determine both $^{18}O/^{16}O$ and $^{17}O/^{16}O$ (see Clayton et al. [8] for details). In cases where only $\delta^{18}O$ values are reported, CO_2 was used as the mass spectrometer gas. Isotopic compositions are reported in the δ-notation, as permil (‰) deviations from the SMOW standard.

3. Results and discussion

3.1. General features

The oxygen isotopic compositions of all samples are given in Tables 1 and 2, and are shown in Fig. 1 for those samples for which both $\delta^{18}O$ and $\delta^{17}O$ are available. Several gross features are evident in the data. Except for samples of C2 matrix, and a single Allende inclusion, all of the meteorite data points in Fig. 1 lie close to a single mixing line which is distinctly unlike the terrestrial mass-fractionation line. On the basis of less precise data, Clayton et al. [1] reported a slope of unity for this mixing line. A least-squares straight line through the data of Fig. 1 has a slope of 0.94 $\pm$ 0.01 (2σ). It is conceivable that systematic errors in the δ^{17}determinations are large enough that the apparent departure from unity is insignificant. In any case, an extrapolation of the mixing line passes very nearly through pure $^{16}O(\delta^{18}O = \delta^{17}O = -1000‰)$.

There is no *simple* association between the magnitude of the ^{16}O enrichment and the chemical or mineralogical composition of the sample, although some important regularities are observed in Allende inclusions, which are discussed below.

The data at the upper end of the mixing line do not extend all the way to the terrestrial fractionation line. Thus *all* the carbonaceous chondrite whole rocks and subsamples are "anomalous" to some extent. Whole-rock analyses of the C3 meteorites lie near 0‰ in $\delta^{18}O$, whereas the intersection of the carbonaceous chondrite line with the terrestrial line is at about +10‰ This difference implies a 1% excess of ^{16}O in the C3 carbonaceous chondrites relative to the earth. No systematic differences in whole-rock isotopic compositions have been observed between the C3O and C3V sub-types.

3.2. Allende inclusions – observations

The samples of Allende include representatives of various classes: the coarse-grained type A (melilite + spinel ± diopsidic pyroxene) and type B (Ti-Al-rich pyroxene + spinel + mililite + anorthite) inclusions of Grossman [3], the fine-grained aggregates (pyroxene + spinel + grossular + feldspathoids) described by Clarke et al [9] and Grossman et al [10], the amoeboid aggregates (olivine + pyroxene + feldspathoids) of Grossman and Steele [11], dark grey or black xenoliths (olivine) and chondrules (olivine).

The heterogeneous distribution of oxygen isotopes is shown by analyses of mineral fractions of individual inclusions. Data for 22 inclusions, chrondrules and matrix samples of Allende are shown in Figs. 2 and 3. Ten of the inclusions were separated into various mineral fractions, primarily by density differences. It is seen that all inclusions have large internal variations in $\delta^{18}O$ and $\delta^{17}O$, with 30–40‰ ranges being common The fine-scale heterogeneity of isotopic composition is proof that the depletions of the heavier isotopes did not result from particle bombardment subsequent to formation of the inclusions. The subsamples all lie along the mixing line, and chemical isotope fractionation between minerals, which is expected to be less than 1‰ in $\delta^{18}O$ for the high-temperature phases, is masked by the very large non-chemical effects.

Several regular features can be seen in the isotopic compositions: spinel samples are invariably enriched in ^{16}O; pyroxene is almost invariably enriched in ^{16}O; melilite is always the least enriched in ^{16}O;

TABLE 1

Oxygen isotopic compositions of minerals from Allende

Sample No.	Fig. No. *	Inclusion type	Density (g/cm^3)	Minerals **	$\delta^{18}O$ (‰)	$\delta^{17}O$ (‰)
A13S4	1	B	2.92–3.12	Me	+1.6	–1.9
			3.32–3.42	*Px*, Sp	–38.2	–39.8
			3.47–3.77	Sp from Me	–38.0	–39.3
			3.47–3.77	Sp from Px	–41.0	–42.3
A1 15	2	B	2.82–3.08	Me	–0.1	–4.0
			3.08–3.20	*Me*, Sp	–6.7	–10.2
			3.32–3.42	Px	–34.8	–35.7
			3.42–3.52	Px, Sp	–39.0	–40.6
A16S3 (rim)	3	B	W.R.	Px,Gr, Ol, Sp	–23.1	–26.1
			<3.12	Px, So, Ne, Gr, Sp	–1.8	–6.1
			3.12–3.26	Ol, Px	–27.8	–31.0
			3.26–3.32	*Px*, Ol	–35.8	–38.2
			3.32–3.39	*Px*, Sp	–32.1	–35.2
			3.39–3.47		–26.7	–29.8
			>3.47		–30.7	–32.8
A16S3 (core)			W.R.	Px, Ol, Sp	–36.6	–38.8
			3.12–3.26	*Ol*, Px	–34.3	–36.3
			3.26–3.32		–39.8	–41.8
			3.32–3.39	Px, Sp	–38.7	–40.8
			>3.47	Sp, Px	–35.7	–37.8
W.U. (rim)	4	B	W.R.	Me, Px, Sp	–8.4	–12.4
(rim)			W.R.		–10.5	–14.0
(center)			W.R.	Px, Sp, Me	–14.3	–17.8
(center)			W.R.		–14.7	–17.9
(center)				Px	–30.7	–32.4
A1 N0-2-05	5	A-B	3.00–3.20	Me	–0.3	–4.2
			3.20–3.32	Me, Sp, Px	–10.9	–14.2
			3.32–3.42	*Px*, Sp	–6.6	–10.1
			>3.42	*Sp*, Px	–28.4	–32.2
A1 N0-1-16	6	A	2.88–3.20	*Me*, Sp, Gr	–1.8	–5.6
			3.20–3.42	Me, Sp	–9.6	–13.1
			3.42–3.52	*Sp*, Me, Gr	–16.7	–19.1
			3.52–3.61	*Sp*, Gr	–35.3	–36.8
A1 N0-1	7	A	W.R.		–10.3	–14.3
			<2.88		+1.3	–3.3
			2.88–3.20	*Me*, Gr	–2.5	–6.8
			3.12–3.20	Me, Gr	–4.8	–8.9
			3.20–3.32	Gr, Me, Hi	–9.4	–13.3
			3.32–3.42	Gr, Hi, Sp, Me	–16.6	–20.1
			3.42–3.52	Gr, Hi, Sp	–18.6	–21.0
			>3.52	Hi, Pe, Sp	–24.3	–26.5
A1 N0-8-11	8	fine-pink	<3.20	Px, So, Ne	–10.4	–14.3
			3.20–3.36	Px, Sp, Gr	–13.2	–17.2
			3.36–3.47	Px, Sp, Gr	–10.9	–15.0
			>3.52	*Sp*, Gr, Px	–26.7	–29.6
A1 N0-9	9	fine-white	<3.20	Ne, Px, Sp	–5.4	–9.3
			3.20–3.36	Px, Ne, Sp	–10.2	–13.8
			3.36–3.52	Px, Sp	–11.9	–15.7
A16S1	10	amoeboid	<3.08	Ol, Ne, So	–7.3	–11.2
			>3.08	Ol	–13.9	–17.0

TABLE 1 (continued)

Sample No.	Fig. No. *	Inclusion type	Density (g/cm^3)	Minerals **	$\delta^{18}O$ (‰) =	$\delta^{17}O$ (‰) =
A2S2	11	B		W.R.	−18.5	−22.0
B29S2	11	fine		W.R.	−12.6	−16.3
B32S2	11	fine		W.R.	−6.2	−10.6
C1S2	11	B		W.R.	−1.7	−11.3
C1S3	11	B		W.R.	−3.0	−13.2
D8	11	B		W.R.	−13.5	−17.2
B31M3	11	matrix		W.R.	+2.1	−2.1
A16S4	12	Ol-chondrule	3.30–3.39	*Ol*, Px	+0.3	−3.5
A1HN-GC	12	Ol-chondrule	3.38-3.52	Ol	−2.7	−6.5
			3.52–3.65	Ol	−2.6	−6.5
Ch-L211	12	Ol-chondrule		W.R.	−1.1	−4.7
AR4C		acid residue >1 μm		Sp	−31.9	−33.5
AR4F		acid residue <1 μm		Sp, Cr	−14.9	
A12	12	dark inclusion		W.R.	+3.6	−1.0
A13	12	dark inclusion		W.R.	+4.6	−0.2
A15	12	dark inclusion		W.R.	+2.5	−1.9

* Gives number of mixing line in Fig. 2 or Fig. 3.

** Abbrevations: W.R. = whole rock; Cr = chromite; Gr = grossular; Hi = hibonite; Me = melilite; Ne = nepheline; Ol = olivine; Pe = perovskite; Px = pyroxene; So = sodalite; Sp = spinel. Minerals listed in approximate order of their abundance; italics indicate dominant phase.

olivine may be found throughout the range of observed isotopic compositions. For samples from the white inclusions, there appear to be natural "ends" to the mixing line, the high-^{16}O end being defined by a cluster of pyroxene and spinel samples with $\delta^{18}O$ of about −40‰, and the low ^{16}O end being defined by a cluster of melilite samples with $\delta^{18}O$ of about 0‰.

Further insight into the distribution of isotopic abundances can be derived from the results of analyses of mineral fractions of particular inclusions. A13S4, a photomicrograph of which is shown in Fig. 4, is a coarse-grained type B inclusion consisting predominantly of millimeter-sized crystals of melilite and clinopyroxene and smaller amounts of anorthite. The inclusion is almost circular in cross-section, and the outermost 1.5 mm consists almost entirely of melilite. Included within all other major phases are euhedral crystals of spinel 40–120 μm in size, which are distributed inhomogeneously and without regard for the host mineral. The mineralogy and texture are almost identical to those described for an inclusion ("chondrule") in the Bali meteorite [12]. Mineral separation was carried out in two steps: first a density separation on a 100–300-μm size fraction to yield a melilite and a pyroxene concentrate, then crushing of these concentrates to <25 μm and a second density separation to yield pure melilite and pyroxene fractions, and two spinel fractions – one from the melilite concentrate, the other from the pyroxene concentrate. The purity of the spinel separates was about 95%, as estimated from their silicon content determined by measuring SiF_4 liberated in the BrF_5 reaction. The isotopic compositions of the two spinel fractions, taking into account the small silicate contamination, are the same, whether they were originally enclosed in pyroxene or in melilite. There is a difference of over 40‰ between the melilite crystals and the 40–120-μm spinel crystals included within them. The isotopic composition of the pyroxene is very similar to that of the spinel. These observations place severe constraints not only on the properties of the carrier of the ^{16}O tracer, but on the processes of formation of the Ca-Al-rich inclusions themselves. In particular the observation is incompatible with formation of all the minerals of the inclusion by crystallization from a liquid, unless some strained hypotheses are called upon. Some of these are discussed below.

Inclusion A16S3, shown in Fig. 5, was sampled to

TABLE 2

Oxygen isotopic compositions of C2, C3 and C4 meteorites

Meteorite (class)	Description *	Size fraction (mesh)	Density (g/cm^3)	Other	Mineralogy *	$\delta^{18}O$ (‰)	$\delta^{17}O$ (‰)
Murchison (C2)	matrix		2.83–2.85		hydrous silicates	+12.8	+4.5
	matrix		2.85–2.92		hydrous silicates	+10.9	+3.4
	chondrule				Ol, Px	–0.9	
	dark inclusion				Ol	+3.9	
	chondrules	>150	2.85–3.12		Ol, Px	–17.0	
		0.2–1 mm	2.85–3.30		Ol	–3.7	
		0.2–1 mm	3.30–3.58		Ol	+2.0	
		0.2–1 mm	3.58–388		Ol	+2.6	
		<325	3.18–3.20		*Px*, Ol	–5.5	
		<325	3.20–3.23		Ol, Px	–8.2	–11.2
		<325	3.23–3.26		Ol, Px	–4.8	
		<325	3.26–3.28		*Ol*, Px	–2.9	–6.3
		<325	3.28–3.33		*Ol*, Px	–2.7	
Murray (C2)	matrix		<2.8		hydrous silicates	+11.3	+3.2
	matrix		2.6 –2.8		hydrous silicates	+10.9	+3.0
		<100	3.17–3.24	non-mag.		–6.9	–9.5
Grosnaja (C3)	W.R.					+2.1	
	white fragments				Ol	–22.4	
		150–325	3.00–3.19	non-mag.	Ol	–2.7	
		150–325	3.19–3.29	non-mag.	*Ol*, Px	–7.3	
		150–325	3.29–3.43	non-mag.	*Ol*, Px	–13.3	
		150–325	3.68–3.89	non-mag.	Ol	+5.9	
		<325	3.15–3.29	non-mag.	Ol	–6.8	
		<325	3.29–3.43	non-mag.	*Ol*, Px	–10.0	
		150–325	3.29–3.43	mag.	Ol	+0.1	
		150–325	3.43–3.55	mag.		+2.6	
		150–325	3.55–3.68	mag.		+4.9	
		150–325	3.68–3.89	mag.		+5.8	
		<325	3.29–3.43	mag.		+1.0	
		<325	3.68–3.89	mag.		+6.6	
Ornans (C3)	W.R.					+0.4	
		<325	3.13–3.23	non-mag.	*Ol*, Px	–6.1	
		<325	3.23–3.33	non-mag.	*Ol*, Px	–6.5	–9.5
		<325	3.33–3.43	non-mag.	*Ol*, Px	–8.7	
		<325	3.43–3.58	non-mag.	*Ol*, Px	–7.0	
		<325	3.58–3.72	non-mag.	Ol	–2.6	
		<325	3.72–3.88	non-mag.	Ol	+0.6	
		<325	3.13–3.23	mag.	Ol	–2.1	–5.2
		<325	3.23–3.33	mag.	Ol	–3.2	
		<325	3.33–3.43	mag.	Ol	–2.7	–6.5
		<325	3.43–3.55	mag.	Ol	–2.8	–6.4
		<325	3.58–3.72	mag.	Ol	–2.1	–5.9
		<325	3.72–3.88	mag.	Ol	–0.9	–5.1
Vigarano (C3)	W.R.					+0.8	
		100–325	3.15–3.20	non-mag.	*Ol*, Px	–6.5	
		100–325	3.20–3.23	non-mag.	*Ol*, Px	–5.2	
		100–325	3.23–3.26	non-mag.	*Ol*, Px	–4.7	
		100–325	3.26–3.33	non-mag.	*Ol*, Px	–4.4	–7.9
		100–325	3.33–3.43	non-mag.	*Ol*, Px	–8.7	
		<325	3.33–3.43	mag.	*Ol*, Px	+1.2	

TABLE 2 (continued)

Meteorite (class)	Description *	Size fraction (mesh)	Density (g/cm^3)	Other	Mineralogy *	$\delta^{18}O$ (‰)	$\delta^{17}O$ (‰)
Warrenton (C3)	W.R.					−0.6	
		<325	3.23–3.33		Px, Ol	−3.9	
		<325	3.33–3.48		Ol, Px	−3.4	
		<325	3.48–3.58		*Ol*, Px	−5.1	
		<325	3.58–3.72		*Ol*, Px	−4.7	
		<325	3.72–3.88		*Ol*	−1.1	
Coolidge (C4)	W.R.					−1.4	−5.2
Karoonda (C4)	W.R.					−1.2	−5.3
	chondrules					−3.2	−6.7
		325–500	2.68–2.78		Pc	+2.2	−3.1
		<500	3.38–3.47		*Ol*, Px	−0.1	−4.4
		<500	3.58–3.64		Ol	−2.4	−5.9
						−2.7	−6.3
		<500	3.64–3.83		Ol	−1.8	−5.8
		<500	4.2		Mt	−3.6	−6.1

* Abbrevations: W.R. = whole rock, Ol = olivine, Px = pyroxene; Mt = magnetite. Minerals listed in approximate order of their abundance; italics indicate dominant phase.

investigate the interaction between the inclusion and its surroundings, either in space before incorporation into the meteorite, or with the meteoritic matrix after accretion. The inclusion is of irregular shape, and is about 15 mm across. The interior of the inclusion is a greyish-tan color, and consists of clinopyroxene with poikilitically enclosed rounded grains of forsteritic olivine and spinel. The outermost millimeter of the inclusion is much finer-grained and lighter in color, and contains nepheline, sodalite and grossular in addition to the minerals found in the interior. The matrix immediately adjacent to the inclusion is very dark and free of large crystals or chondrules.

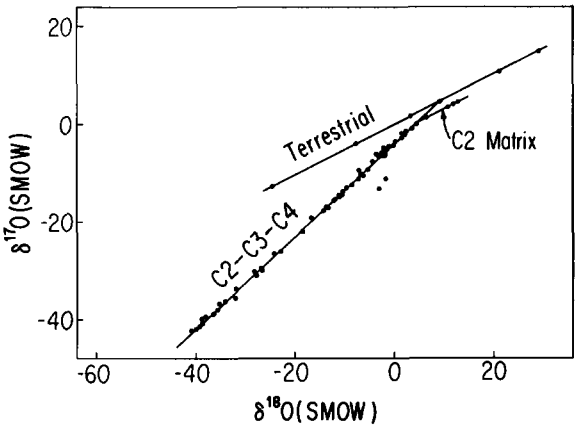

Fig. 1. Graph of $^{17}O/^{16}O$ vs. $^{18}O/^{16}O$ for (1) a variety of terrestrial samples (rocks, minerals, waters), showing the slope-1/2 mass-fractionation line expected for mass dependent isotope effects, (2) separated fractions from the Allende meteorite and eight other carbonaceous chondrites (classes C2, C3 and C4), showing various mixtures of "normal" oxygen and an ^{16}O-rich component, and (3) a second mass-fractionation line for matrix material from C2 meteorites.

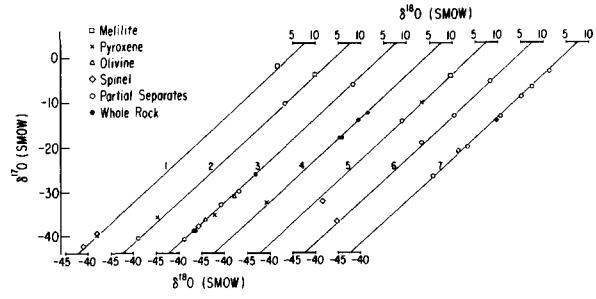

Fig. 2. Oxygen isotopic compositions of separated phases from seven coarse-grained inclusions from Allende: lines 1–4 from type B, lines 6 and 7 from type A, line 5 from an intermediate type (see Table 1 for details). In all cases, the line is taken from Fig. 1, a best straight-line fit to the data from all the meteorites discussed in this paper.

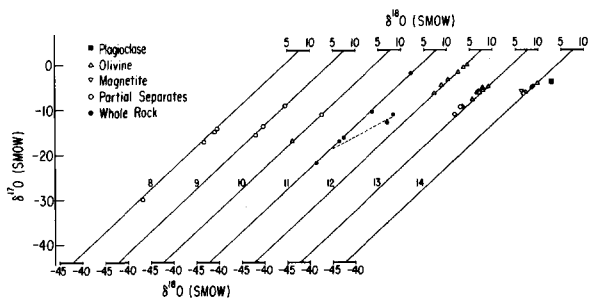

Fig. 3. Oxygen isotopic compositions of various carbonaceous chondrite samples, as follows: lines 8 and 9 are Allende fine-grained inclusions; line 10 is an Allende amoeboid olivine aggregate; line 11 shows whole-rock analyses of Caltech Allende samples [5]; line 12 shows olivine-rich Allende samples; line 13 shows samples of Murray, Ornans and Vigarano; line 14 shows samples of Coolidge and Karoonda (see Tables 1 and 2 for details). In all cases, the line is taken from Fig. 1. All the data points lie close to the mixing line except two splits of the Caltech sample C1 [5]. A hypothetical mass-fractionation line for sample C1 is shown as a dashed line next to mixing line 11.

All of the minerals from the interior of the inclusion have very low $\delta^{18}O$ and $\delta^{17}O$ values, ranging from −35‰ to −40‰. The whole-rock rim sample has less negative δ-values, and it is seen from the mineral analyses that this is due to relatively high δ-values in the lowest-density fraction, which contains the phases presumably formed at lower temperatures: nepheline, sodalite and grossular. It can be inferred that inclusion Al6S3 had rather uniformly low δ-values prior to the reactions which led to formation of the lower-temperature phases. The data presented here do not distinguish between reactions before or after embedding the inclusion in the meteoritic matrix.

The isotopic compositions of the major mineral phases in coarse-grained type A inclusions are about the same as in coarse-grained type B inclusions. Compare, for example, melilite and spinel from A1 N0-1-16 (Fig. 2, line 6) with the corresponding minerals from A1 15 (Fig. 2, line 2). However, because of the large modal abundance of low $-\delta^{18}O$ clinopyroxene typically found in the type B inclusions, the magnitude of the ^{16}O anomaly for the inclusion as a whole is considerably greater for type B than for type A. Based on the estimates of mineral proportions given by Grossman [3] and by Grey et al. [5] the whole-inclusion $\delta^{18}O$-values for type A inclusions would be about −8‰, while the values for type B inclusions would range between −15‰ and −30‰. The two fine-grained inclusions analyzed in this work (A1 N0-8-11 and A1 N0-9) have intermediate δ-values around −15‰, as do some of the samples from the Caltech collection (Fig. 3, line 11). Although pure mineral fractions were not generally obtained from fine-grained inclusions, the impression from analyses of partial separates is that their intermediate δ-values are the result of mixing of low-anomaly phases (nepheline, sodalite, grossular) with high-anomaly phases (spinel and possibly clinopyroxene). The single example of an amoeboid olivine aggregate reported here also has an intermediate $\delta^{18}O$-value of about −14‰, but a value as low as −26‰ has been reported for another amoeboid olivine aggregate [1].

Olivine chondrules, and dark grey inclusions which are composed primarily of iron-rich olivine, have the lowest content of ^{16}O-rich component of any samples of Allende yet analyzed. Even these lie distinctly below the terrestrial fractionation line (Fig. 3, line 12).

Ca-Al-rich inclusion C1 is the only sample of Allende which lies appreciably off the isotopic mixing line. This sample was part of the collection analyzed for Rb and Sr by Gray et al. [5]. Its major and trace element chemical compositions and its strontium isotope abundances were not found to be unusual. Its principal mineral phases are coarse-grained melilite, clinopyroxene and spinel, as in type B Ca-Al-rich inclusions. Lee and Papanastassiou [6] and Lee et al. [13] found sample C1 to have a unique magnesium isotopic composition, having apparent large mass-fractionated enrichments of the heavy isotopes: $\delta^{26}Mg \sim +59‰$ and $\delta^{25}Mg \sim +30‰$ relative to terrestrial magnesium. The observed oxygen isotopic compositions could also be interpreted as mass-fractionation effects, as indicated by the dashed line in Fig. 3. The starting material could have had a "typical" composition for an Allende white inclusion ($\delta^{18}O \sim -15‰$, $\delta^{17}O \sim -18‰$). The mass-fractionation enrichment would then be about 12‰ for $\delta^{18}O$ and 6‰ for $\delta^{17}O$. One hypothetical process which might lead to such large isotope effects is evaporation, with heavy isotopes becoming enriched in the residue. However, such large fractions of the

Fig. 4. Photomicrograph of A13S4, a coarse-grained type B inclusion from Allende. The outer 1.5 mm border consists of radially oriented melilite crystals, with the content of included spinel increasing inwards. The interior of the inclusion is predominantly coarsely crystalline clinopyroxene, melilite and anorthite, all containing euhedral crystals of spinel. The field of view is 22 mm × 17 mm.

starting material need to be removed to produce the observed effects (at least 80% of the magnesium and 10% of the oxygen) that major effects on the chemical and mineralogical compositions should be evident. In fact, because this inclusion does not appear unusual in its contents of Rb and Sr [5] or Mg and Al [13] or in its mineralogy, a starting material totally unlike the usual refractory inclusions would have to be postulated. Inclusion C1 is internally heterogeneous in oxygen isotopic composition, as shown by the analyses of two splits of the same powder (C1S2 and C1S3). The two samples do not appear to lie on a single mass-fractionation trend. Inclusion C1 remains an enigma.

3.3. Allende inclusions – discussion

Carrier phases. If the mineral phases in Allende inclusions had co-crystallized at high temperature either from a liquid or from a vapor, they would be expected to have small differences in $\delta^{18}O$ (on the order of 1‰ or less) and to lie on a slope-1/2 fractionation line on the $\delta^{17}O$ vs. $\delta^{18}O$ graph. None of the inclusions analyzed shows such behavior. One possible explanation might be that the various minerals formed in different regions of space, from gases and/or solids of different oxygen isotopic composition, and were subsequently assembled into the in-

Fig. 5. Photomicrograph of A16S3, an atypical, moderately coarse-grained inclusion from Allende. The two separate areas seen in the thin section merge into one in the opposite face of the saw-cut from which samples were taken. The core consists of olivine and spinel, poikilitically enclosed by clinopyroxene; the "altered" rim also contains nepheline, sodalite and grossular (identified by X-ray patterns). The two white areas near the center are holes in the section. The field of view is 22 mm × 17 mm.

clusions now found in the meteorite. Yet the rare earth element data for similar inclusions show complementary patterns for melilite and pyroxene, implying a crystal chemical control on the trace element distribution [4,14,15]. Some textural evidence is interpreted in terms of crystallization from a melt [3, 12,16]. Perhaps the ^{16}O-rich component is present in a minor phase, included preferentially in pyroxene and spinel, which has not yet been observed except through its isotopic signature. If this is the case, the *minimum* concentration of the exotic phase in pyroxene and spinel is 5%, for a pure ^{16}O compound. Any less extreme isotopic composition would require greater concentrations which should make visual detection easier. To have avoided detection by optical, X-ray and chemical techniques, the exotic phase

would be expected to have grain size < 1 μm, and to be composed of some of the same major elements as the host minerals: magnesium, aluminium, silicon, calcium or titanium. If the inclusions were once molten, these elements would have had to be combined in a compound which does not melt or exchange rapidly with a silicate melt at high temperatures. Possible candidates might be corundum, spinel or perovskite [17]. It is difficult to see how this explanation would account for the enormous heterogeneity of distribution within individual inclusions, with similar contents in pyroxene and spinel, and virtual exclusion from melilite. None of the proposed carrier minerals would account satisfactorily for the ^{16}O excesses observed in other carbonaceous chondrites in pure forsteritic olivine. (It should be noted, however, that C2 olivines contain significant amounts of Ca-Al-rich *glass* which might be an ^{16}O carrier [18].)

Partially molten condensates. Grossman and Clark [19] considered the possibility that a temperature range of stable liquids might be encountered in the course of equilibrium condensation from the solar nebula. They concluded that such a field would not be encountered at pressures below 2.2×10^{-3} atm, but that the system would approach within 50° of the solidus at 10^{-3} atm during the condensation of diopside at a temperature of 1450 K, (1442 K according to more recent calculations) which causes the composition of the solid condensates to become much richer in Mg and Si. The pyroxene actually observed as a major phase in the type B coarse-grained inclusions is, of course, not diopside, but fassaite containing large amounts of trivalent titanium [20]. Because of the lack of appropriate thermodynamic data it was not possible for Grossman and Clark to estimate accurately the effect of the aluminium and titanium content of the clinopyroxene in their computations. These elements might well stabilize the solid phase and raise its condensation temperature by some tens of degrees. Higher condensation temperatures, and increased probability of intersecting the solidus would also result if a higher nebular gas pressure prevailed. For example, the equilibrium condensation temperature for diopside increases from 1442 to 1510 K for a pressure increase from 10^{-3} to 10^{-2}atm. Thus there is a significant likelihood that the initially solid condensates would enter the field of stable liquids (with monotonic cooling) due to the large change in bulk composition of the solids associated with the condensation of pyroxene.

The development of a liquid phase during equilibrium condensation of a solar nebular gas may be illustrated by consideration of a system containing the four major components of the refractory phases: MgO, CaO, Al_2O_3, SiO_2, with H_2 as the major component of the gas phase. Grossman and Clark [19] have shown that liquids will not be encountered if the nebular pressure is $<10^{-3}$ atm, so that we shall examine the behavior at a higher pressure, i.e., 10^{-2} atm. The first major phase to condense is corundum, at 1810 K. At 1705 K, corundum begins to react with calcium and silicon from the vapor to give gehlenite. The gehlenite begins to incorporate magnesium and more silicon at about 1600 K, producing melilite solid solutions; at about this same temperature, the remaining corundum reacts with magnesium from the vapor to give spinel. The melilite-spinel assemblage cools to 1510 K, with continuously increasing åkermanite content of the melilite. At 1510 K, the reaction: Me + v → Di + Sp begins. This reaction causes a large change in the bulk composition of the condensed solids at almost constant temperature [19], carrying the composition of the solids into the tetrahedron bounded by anorthite, melilite, spinel and diopside [21, fig. 9]. Within this field, a liquid phase is stable above 1500 K [21]. Therefore one of the solid phases must disappear in an invariant reaction:

$$\text{Me} + \text{Di} + \text{Sp} + \text{v} \rightarrow \text{Di} + \text{Sp} + \text{l} + \text{v}$$

The composition may reach a point at which diopside also enters the liquid, leaving only spinel + liquid + vapor. Then upon cooling, the liquid precipitates clinopyroxene, anorthite and melilite [21].

The situation is more complicated if TiO_2 is included as an additional component. In the equilibrium condensation scheme of Grossman [17], titanium is essentially completely condensed between 1680 and 1600 K (at a total pressure of 10^{-3} atm) as perovskite. At 1393 K, titanium is reduced in part to Ti^{3+}, giving Ti_3O_5. Although Ti_3O_5 is not observed as a phase in Allende inclusions, titanium *is* present as a major constituent in the clinopyroxene of type B inclusions and is largely trivalent [20]. Hence, it is possible that the perovskite which condensed at high temperature later reacts with subsequent condensates

to form clinopyroxene, as shown schematically by the equation:

$$2\ CaTiO_3 + SiO_{(g)} + SiO_2 + Al_2O_3 \rightarrow 2\ CaTi^{3+}AlSiO_6$$

Seitz and Kushiro [22] have determined experimentally the melting relations for one Allende Ca-rich inclusion. The details of their experiment may not apply directly to the arguments here concerning coarse-grained type B inclusions, since their study apparently involved a fine-grained inclusion, which is more sodium- and iron-rich. However, the qualitative features of the phase diagram are probably applicable to the coarse-grained inclusions because the CaO, Al_2O_3, MgO and SiO_2 contents of the fine-grained inclusion used by them are very similar to those of coarse-grained inclusions [9]. At 1 atm, melting begins at ~1450 K, with melilite being the first phase to disappear, followed by plagioclase then clinopyroxene. Between 1500 and 1725 K, spinel is the only crystalline phase. Thus a plausible paragenesis for type B inclusions, maintaining equilibrium, and under continuously falling temperatures, is as follows:

(1) condensation of corundum, beginning at 1810 K
(2) condensation of perovskite beginning at 1750
(3) reaction of corundum and vapor to give gehlenite ~1705
(4) reaction of corundum and vapor to give spinel ~1610
(5) reaction of perovskite, melilite and vapor to give clinopyroxene >1520
(6) melting of melilite and some or all of the clinopyroxene ~1520
(7) crystallization of clinopyroxene, anorthite and melilite from the melt ~1500

This sequence would account for (1) the control of major- and trace-element chemistry of the inclusion as a whole by gas-solid reactions [17], (2) the complementary rare earth distribution between melilite and pyroxene [4,14], (3) the textural relationships, including the ubiquitous inclusion of spinel within melilite and pyroxene and the often-seen radial compositional zoning of melilite. It may well be that one of the distinctions between coarse-grained inclusions and fine-grained inclusions in Allende is that the former passed through a stage of partial melting whereas the latter did not. Another distinctive feature of the coarse-grained inclusions is their large size compared with the ordinary chondrules in Allende [9]. This feature may result from the increased efficiency of accretionary growth while in the liquid state.

There remains the problem of understanding how the large oxygen isotope heterogeneity could persist through the proposed stages of melting and recrystallization. From the phase relations described above, the only mineral formed directly from the vapor which does not undergo subsequent melting is spinel. Spinel is also the phase which consistently shows the largest ^{16}O excess. Thus it is possible that spinel is a carrier of the isotopic anomaly (perhaps inherited from pre-solar corundum grains). If so, then diffusion must be slow enough that the spinel grains did not equilibrate with the melt during the time the inclusions were molten. On the basis of self-diffusion coefficients for oxygen in spinel [23], Nagasawa et al. [4] have estimated that isotopically anomalous spinel grains, 1 μm in diameter, would become homogenized by diffusion and exchange with surrounding minerals in about one year at 1500 K. This may not be an unreasonably short cooling time for the initial cooling in an almost grain-free cloud [24].

A more difficult problem seems to be the explanation of large isotopic anomalies in pyroxene. It is tempting to speculate that pre-solar perovskite may have been an ^{16}O carrier, which somehow brought its oxygen as well as its titanium into the clinopyroxene. This mechanism would imply a correlation between the size of the ^{16}O anomaly and the titanium content in clinopyroxenes. The data available are insufficient to test such a hypothesis, but the limited evidence suggests a correlation in the opposite sense: a decreased ^{16}O anomaly associated with high titanium content, as seen in inclusion A1 N0-2-05.

Molecular carriers. Inclusion A1 N0-2-05 is a representative of a class of inclusions which does not fit easily into either of the two groups of coarse-grained inclusions described by Grossman [3]. It is composed more than 90% of melilite, like a type A inclusion, but does contain a small amount of high-Ti fassaite, normally absent in type A and abundant in type B inclusions. The fassaite is of the very high-Ti group discussed by Mason [25]. Other examples of such inclusions are D7 of Gray et al. [5], which has the lowest $^{87}Sr/^{86}Sr$ yet measured, TS18F1 of Grossman [3], USNM 3848 of Dowty and Clark [20],

and sample A of Fuchs [26]. Nagasawa et al. [4] classified A1 N0-2-05 as a type A inclusion and reported a relatively flat rare earth pattern for the melilite fraction (except for a positive europium anomaly).

Although the oxygen isotopic compositions of the melilite and spinel fractions of A1 N0-2-05 are similar to values found in both type A and type B inclusions, the clinopyroxene has a composition which is much less ^{16}O-rich than that found in the more common type B inclusions, such as A13S4 and A1 15.

The titanium content of pyroxenes in this group of inclusions is so high (16–18% as TiO_2) that even a few modal percent accounts for most of the titanium in the inclusion. These inclusions appear to be transitional in degree of condensation between type A (growth arrested prior to condensation of the components of diopside) and type B (growth continued through condensation of diopside). If this indeed represents the sampling of a sequence of processes, the implication is that the ^{16}O anomaly found in fassaite in type B inclusions was introduced along with the condensation of the components of diopside, after condensation of Ca, Al and Ti were essentially complete. Unless we postulate a chance influx of new ^{16}O-carrying refractory particles at this stage, the only feasible ^{16}O carrier would seem to be molecular SiO, which is a stable compound in a gas of solar composition up to very high temperatures, and is the principal silicon-containing compound until the condensation of forsterite [17]. The rate of oxygen isotope exchange between $SiO_{(g)}$ and $CO_{(g)}$ (the principal oxygen compound in the solar nebula at high temperatures) may be slow, since both compounds have very high bond energy, implying a very high activation energy for exchange. An order of magnitude estimate of the rate of isotopic exchange between SiO and CO in the gas phase can be made, using conventional collison theory and assuming an activation energy similar to that found for exchange between CO molecules in the presence of argon [27], For a nebular pressure of 10^{-3} atm, and a temperature of 1500 K, the mean lifetime of a labelled SiO molecule is about ten years. The appropriate activation energy, in the absence of a massive collision partner such as argon, may be considerably higher, giving a smaller exchange rate. Thus, SiO molecules, perhaps formed with ^{16}O excesses in a supernova shell, might persist with their isotopic labels until incorporated into silicon-bearing solids or liquids. If SiO is postulated as an ^{16}O carrier, however, we must reckon with the fact that the fate of most SiO molecules is incorporation into olivine [17], which constitutes the major constituent of chondrites and of the stony parts of planets. Why do they not show large ^{16}O excesses relative to the nebular oxygen? In fact, they may have such excesses, since we have no sample of the nebular reservoir for comparison. It *is* known that the various meteorites and planets have *different* proportions of the ^{16}O-rich component [8], but the absolute amounts are unknown. Furthermore, the exchange between molecular SiO and CO and H_2O molecules is probably much faster when it can take place heterogeneously on solid surfaces formed as condensation proceeds, so that large anomalies are not found in lower-temperature condensates.

None of the hypotheses involving SiO as an ^{16}O carrier would have any bearing on the observation of ^{16}O excesses in spinel, which requires a separate carrier, but they would be applicable to the understanding of ^{16}O excesses in forsterite and enstatite in C2 and C3 chondrites.

Diffusion effects. A different class of models to explain the heterogeneous isotopic distribution within Allende inclusions postulates an initial high-temperature origin, all phases being equilibrated and having a large isotope anomaly, with δ^{18}O near –40‰. Subsequent oxygen exchange might then occur with either the solar nebular gas or with the matrix material of the meteorite, both of which had more nearly "normal" isotopic abundances. If such exchange were only partial, its extent being controlled by diffusion rates, then minerals in which oxygen diffusion is rapid would approach the exchange reservoir in isotopic composition, while those in which diffusion is slow would be little changed from their initial compositions. This might be an attractive explanation if it should turn out that oxygen diffusion in melilite is much faster than in pyroxene and spinel. This mechanism also requires that oxygen diffusion be faster than cation diffusion in melilite, since this mineral usually retains compositional zoning with respect to Al and Mg+Si. A mathematical formulation based on a similar model but postulating pure ^{16}O solids has been given by Blander and Fuchs [16]. Exchange processes such as those considered here may help to

explain the isotopic heterogeneity within some inclusions, but do not help to explain the origin of the initial isotopic anomaly.

3.4. Other carbonaceous chondrites

Although most of the data given in Table 1 for Murchison, Murray, Grosnaja, Ornans, Vigarano, and Warrenton are for $\delta^{18}O$ only, a sufficient number of $\delta^{17}O$ measurements have been made to show that anhydrous silicates from all of these C2 and C3 meteorites fall on the the same mixing line as do the separates from Allende (line 13 in Fig. 3). The same holds for the C4 meteorites, Coolidge and Karoonda (line 14 in Fig. 3). This confirms the results obtained earlier using carbon dioxide as the mass spectrometer gas on different samples of these same meteorites [1]. The $\delta^{18}O$ data in Table 1 are given to show that these meteorites also are extremely heterogeneous with respect to their oxygen isotopic composition. It may well be that they would show as great a range of composition as Allende if it were possible to sample them in an analogous way.

The bulk $\delta^{18}O$ of all of the C3 meteorites analyzed (including Allende) is about $0 \pm 1‰$. The internal variation of isotopic composition is roughly correlated with the mineral chemistry: very negative δ-values are generally associated with magnesium-rich olivine and pyroxene, with more positive δ-values in the iron-rich minerals. This parallels the observations made on olivine and pyroxene in Allende. Furthermore, higher $\delta^{18}O$ values are found for magnetic fractions of a given density range, suggesting a connection between the sulfide mineralization processes and decrease in the isotope anomaly. Thus the lower-temperature secondary processes in all meteorites of this group tend to reduce the magnitude of the anomaly.

The question arisies as to whether there has been sufficient internal redistribution of isotopes within any of the C3 or C4 meteorites to move the data points off the mixing line due to chemical isotope effects. Such internal equilibration has clearly been seen for petrographic types 4–6 in the ordinary chondrites [8]. Data for various mineral fractions of Karoonda (C4) are given in Table 2 and are plotted in Fig. 6. The range of isotopic composition for different olivine fractions clearly shows that the meteorite as a whole has not been internally equilibrated.

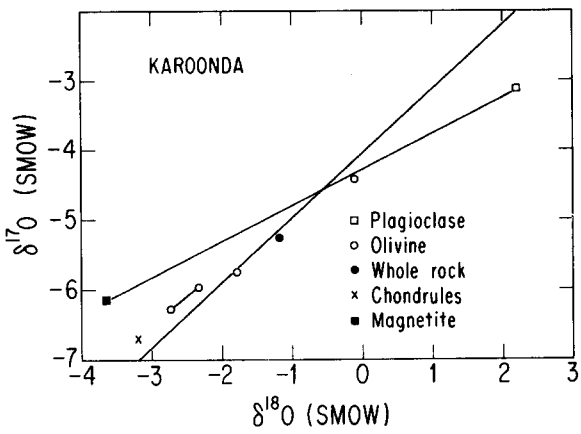

Fig. 6. Expanded three-isotope graph for separated phases of Karoonda (C4). The olivine fractions and the bulk meteorite lie along the ^{16}O mixing line defined by the C3 meteorites. Plagioclase and magnetite are well off this line, and the tie-line between them has a slope of 1/2, consistent with an equilibrium isotopic fractionation between these two phases. The implied temperature of metamorphism is about 580°C.

However, the plagioclase and magnetite data fall well off the ^{16}O mixing line, and show the slope-1/2 relationship expected for equilibrium between these two phases. Perhaps coincidentally, the most magnesian of the olivine fractions also lies on this plagioclase-magnetite line. If these phases have been equilibrated during metamorphism, a metamorphic temperature can be estimated from the magnitudes of the isotopic fractionations using the calibrations given by Anderson et al. [28]. Concordant "isotopic temperatures" at 590 and 580°C are derived from the plagioclase-magnetite pair and the plagioclase-olivine pair respectively.

3.5. C2 and C3 matrix

It is not easy to define the matrix of the C3 meteorites in such a way as to distinguish it from other features such as dark lithic fragments. The dominant phase is a very fine-grained olivine. The oxygen isotopic composition of C3 matrix appears virtually indistinguishable from that of the bulk meteorite.

The matrix of C2 chondrites is readily distinguished from the chondrules, mineral fragments, etc., in that it is composed primarily of a fine-grained, hydrous layer-lattice silicate, whereas the chondrules and mineral fragments are primarily olivine and pyroxene. The

oxygen isotopic compositions of the olivine and pyroxene of C2 meteorites all fall on the line of ^{16}O enrichment, along with minerals of the C3 group. The C2 matrix samples, on the other hand, define an entirely different trend, which follows a slope-1/2 line, and is, therefore, presumably a mass-fractionation trend. Further discussion of C2 matrix and its relation to C1 chondrites is given elsewhere [29]. Suffice it to say for our present purposes that the hydrous matrix and the anhydrous phases of C2 chondrites cannot be directly related to one another in the sense that one could be produced from the other by chemical processes. In particular, C2 chondrules cannot be made by melting C2 matrix material [30].

3.6. Relationship to isotopic anomalies in other elements

Clayton et al. [1] noted that ^{16}O excesses of nucleosynthetic origin might be expected to be closely correlated with isotopic anomalies in other light elements, such as magnesium and silicon. Subsequently, isotopic anomalies in magnesium were found [31,6,13] in Ca-Al-rich inclusions of the Allende meteorite, but these appear to be the result of ^{26}Al radioactive decay, rather than the direct consequence of nucleosynthesis. On a mineral-by-mineral basis, there is no positive correlation between ^{16}O excess and ^{26}Mg excess [6]. In fact, one of the samples with a large excess of ^{26}Mg, BG-2-6 [13], is composed of grossular and hedenbergite, neither of which is expected among the high-temperature condensates. As noted above, grossular usually appears to be a product of interaction between the primary phases and the surroundings (either in the nebula or in the meteorite parent body), and typically shows no ^{16}O excess relative to the whole meteorite.

The lack of an observable direct nucleosynthetic magnesium isotope anomaly may be understood if all three stable isotopes are produced in the same nucleosynthetic process, such as explosive carbon-burning, as described by Arnett [32]. This situation does not hold for silicon, however, ^{28}Si being formed primarily in explosive oxygen-burning [33], and ^{29}Si and ^{30}Si being produced in explosive carbon-burning. Thus, correlated anomalies in oxygen and silicon are still to be expected, especially if SiO plays a significant role as an ^{16}O carrier.

Xenon of unusual isotopic composition has also been found in Allende, although not apparently associated with the high-temperature phases [34]. We have carried out oxygen isotopic analyses on two of the rare-gas rich residues prepared by Lewis et al. [34]. One sample, consisting primarily of spinel and chromite with grain-size >10 μm, falls on the ^{16}O enrichment line with $\delta^{18}O = -31.9‰$. The other sample, a mixture of carbon, chromite, and spinel, all with grain size <1 μm, has $\delta^{18}O = -14.9‰$, and a higher concentration of rare gases. There is no evident correlation between the rare gas anomalies and the oxygen anomalies.

The isotopically anomalous component of neon, Ne-E [35–37], to which an extrasolar origin has been attributed, appears to be associated only with the low-temperature hydrous silicates of the C1 and C2 chondrites. In this case, the vast chemical difference between neon and oxygen would certainly account for the difference in final location of isotopically anomalous components, even if the two elements had originally acquired their isotopic labels in the same nucleosynthetic event.

4. Conclusions

Of the several "isotopic anomalies" recently reported in various primitive meteorites, the ^{16}O excess provides the strongest evidence for a presolar nucleosynthetic origin, primarily because the number of atoms involved is so great that alternative processes, such as proton bombardment within the solar system, are quantitatively inadequate [38]. It remains as a major mystery, however, that the actual particles which brought the ^{16}O to the solar nebula have not yet been identified, even though they constitute at least 5% of various macroscopic, nearly monomineralic samples. Although several suggestions have been presented here to account for the isotopic and chemical observations, none is completely satisfying. Further evidence may be found by still finer examination of the Allende inclusions. Recent studies have revealed tiny "nuggets" of platinum metals within Allende Ca-Al-rich inclusions [39], demonstrating that many of the trace elements are not entirely contained within the structures of the major

minerals. Uranium and thorium have been observed as major constituents of accessory minerals [40]. A similar mode of occurrence was suggested for oxides of the rare earths [15]. Additonal studies of this sort with the electron microprobe and electron microscope may supply sufficient additional constraints on the mode of origin of the high-temperature inclusions so as to rule out some of the conjectures presented here.

The details of the nucleosynthetic event(s) which produced the ^{16}O excesses will only be revealed if some correlations are observed with isotopic effects in other elements. So far, such correlations have not been found, but some of the promising candidate elements, particularly silicon, have not yet been studied. Anomalies have been sought in calcium and have been found to be less than 0.1% in any isotope ratio (G.J. Wassurburg, personal communication).

The largest ^{16}O excesses measured (~5%) occur in spinel and clinopyroxene separates from several Allende inclusions. The recurrence of about the same value in all of the coarse-grained inclusions measured implies that this limit is a property of the meteorite, and that further sampling of Allende is unlikely to reveal progressively greater enrichments. It is obviously of importance to examine comparable samples from other carbonaceous chondrites, which may have greater refractory element enrichments than those of Allende, in order to look for more extreme isotopic compositions.

Acknowledgements

This research was supported by National Science Foundation grants GA22711 and EAR-74-19038 (R.N.C.), N.A.S.A. grant NGR-14-001-249 (L.G.) and a grant from the Research Corporation (L.G.).

We gratefully acknowledge receipt of meteorite samples from Edward J. Olsen (Field Museum of Natural History), Edward Anders (University of Chicago), Kurt Marti (University of California, San Diego), Robert Walker (Washington University) and G.J. Wasserburg (Calfornia Institute of Technology).

We have benefitted greatly from discussions with many colleagues, including Edward Anders, Richard Becker, Robert Newton and Peter Wyllie.

References

1 R.N. Clayton, L. Grossman and T.K. Mayeda, A component of primitive nuclear composition in carbonaceous meteorites, Science 182 (1973) 485–488.
2 R.N. Clayton, L. Grossman, T.K. Mayeda and N. Onuma, Heterogeneities in the solar nebula, Proc. Soviet-American Conf. on Cosmochemistry of Moon and Planets (in press).
3 L. Grossman, Petrography and mineral chemistry of Ca-rich inclusions in the Allende meteorite, Geochim. Cosmochim. Acta 39 (1975) 433–454.
4 H. Nagasawa, D.P. Blanchard, J.W. Jacobs, J.C. Brannon, J.A. Philpotts and N. Onuma, Trace element distribution in mineral separates of the Allende inclusions and their genetic implications (submitted to Geochim. Cosmochim. Acta).
5 C.M. Gray, D.A. Pananastassiou and G.J. Wasserburg, The identification of early condensates from the solar nebula, Icarus 20 (1973) 213–239.
6 T. Lee and D.A. Papanastassiou, Mg isotopic anomalies in the Allende meteorite and correlation with O and Si effects, Geophys. Res. Lett. 1 (1974) 225–228.
7 R.N. Clayton and T.K. Mayeda, The use of bromine pentafluoride in the extraction of oxygen from oxides and silicates for isotopic analysis, Geochim. Cosmochim. Acta 27 (1963) 43–52.
8 R.N. Clayton, N. Onuma and T.K. Mayeda, A classification of meteorites based on oxygen isotopes, Earth Planet. Sci. Lett. 30 (1976) 10–18.
9 R.S. Clarke, Jr., E. Jarosewich, B. Mason, J. Nelen, M. Gomez and J.R. Hyde, The Allende, Mexico, meteorite shower, Smithsonian Contrib. Earth Sci. (1970) 53 pp.
10 L. Grossman, R.M. Fruland and D.S. McKay, Scanning electron microscopy of a pink inclusion from the Allende meteorite, Geophys. Res. Lett. 2 (1975) 37–40.
11 L. Grossman and I.M. Steele, Amoeboid olivine aggregates in the Allende meteorite, Geochim. Cosmochim. Acta 40 (1976) 149–155.
12 G. Kurat, G. Hoinkes and K. Fredriksson, Zoned Ca-Al-rich chondrule in Bali: new evidence against the primordial model, Earth Planet. Sci. Lett. 26 (1975) 140–144.
13 T. Lee, D.A. Papanastassiou and G.J. Wasserburg, Demonstration of ^{26}Mg excess in Allende and evidence for ^{26}Al, Geophys. Res. Lett. 3 (1976) 109–112.
14 B. Mason and P.M. Martin, Minor and trace element distribution in melilite and pyroxene from the Allende meteorite, Earth Planet. Sci. Lett. 22 (1974) 141–144.
15 L. Grossman and R. Ganapathy, Trace elements in the Allende meteorite, 1. Coarse-grained, Ca-rich inclusions, Geochim. Cosmochim. Acta 40 (1976) 331–344.
16 M. Blander and L. Fuchs, Calcium-aluminium-rich inclusions in the Allende meteorite: evidence for a liquid origin, Geochim. Cosmochim. Acta 39 (1975) 1605–1619.
17 L. Grossman, Condensation in the primitive solar nebula, Geochim. Cosmochim. Acta 36 (1972) 597–619.
18 L.H. Fuchs, E. Olsen and K.J. Jensen, Mineralogy, mineral-chemistry, and composition of the Murchison (C2)

meteorite, Smithsonian Contrib. Earth Sci. No. 10 (1973) 39 pp.
19 L. Grossman and S.P. Clark, Jr., High-temperature condensates in chondrites and the environment in which they formed, Geochim. Cosmochim. Acta 37 (1973) 635–649.
20 E. Dowty and J.R. Clark, Crystal structure refinement and optical properties of a Ti^{3+} fassaite from the Allende meteorite, Am. Mineral. 58 (1973) 230–242.
21 J.F. Schairer and H.S. Yoder, Jr., Critical planes and flow sheet for a portion of the system $CaO–MgO–Al_2O_3–SiO_2$ having petrological applications, Carnegie Inst. Washington Yearb. 68 (1970) 202–214.
22 M.G. Seitz and I. Kushiro, Melting relations of the Allende meteorite, Science 183 (1974) 954–957.
23 K. Ando and Y. Oishi, Self-diffusion coefficients of oxygen ion in single crystals of $MgO–nAl_2O_3$ spinels, J. Chem. Phys. 61 (1974) 625–629.
24 A.G.W. Cameron, The formation of the sun and planets, Icarus 1 (1962) 13–69.
25 B. Mason, Aluminium-titanium-rich pyroxenes, with special reference to the Allende meteorite, Am. Mineral. 59 (1974) 1198–1202.
26 L.K. Fuchs, Occurrence of wollastonite, rhönite and andradite in the Allende meteorite, Am. Mineral. 56 (1971) 2053–2068.
27 A. Bar-Nun and A. Lifschitz, Kinectics of the homogeneous exchange reaction $^{12}C^{18}O + {}^{13}C^{16}O \rightleftharpoons {}^{13}C^{18}O + {}^{12}C^{16}O$. Single-pulse shock-tube studies, J. Chem. Phys. 51 (1969) 1826–1833.
28 A.T. Anderson, Jr., R.N. Clayton and T.K. Mayeda, Oxygen isotpe thermometry of mafic igneous rocks, J. Geol. 79 (1971) 715–729.
29 T.K. Mayeda and R.N. Clayton, Oxygen isotopic composition of C1 and C2 carbonaceous chondrites (in preparation).
30 E. Anders, Conditions in the early solar system, as inferred from meteorites, in: From Plasma to Planet, Proc. 21st Nobel Symp. A. Elvius, ed. (Wiley, New York, N.Y., 1971) 133–150.
31 C.M. Gray and W. Compston, Excess ^{26}Mg in the Allende meteorite, Nature 251 (1974) 495–497.
32 W.D. Arnett, Explosive nucleosynthesis in stars, Appl. J. 157 (1969) 1369–1380.
33 S.E. Woosley, W.D. Arnett and D.D. Clayton, The explosive burning of oxygen and silicon, App. J. Suppl. 26 (1973) 231–312.
34 R.S. Lewis, B. Srinivasan and E. Anders, Host phase of a strange xenon component in Allende, Science 190 (1975) 1251–1262.
35 D.C. Black and R.O. Pepin, Trapped neon in meteorites, II, Earth Planet. Sci. Lett. 6 (1969) 395–405.
36 D.C. Black, On the origins of trapped helium, neon and argon isotopic variation in meteorites, II. Carbonaceous meteorites, Geochim. Cosmochim. Acta 36 (1972) 377–394.
37 P. Eberhardt, A neon-E-rich phase in the Orgueil carbonace ous chondrite, Earth Planet. Sci. Lett. 24 (1974) 182–187
38 D.D. Clayton, E. Dwek and S.E. Woosley, Isotopic anomalies and proton irradiation in the early solar system (submitted to Astrophys. J.).
39 D.A. Wark and J.F. Lovering, Refractory/platinum metal grains in Allende calcium-aluminium-rich clasts (CARC's): possible exotic presolar material (abstract) Lunar Sci. VII (1976) 912–915.
40 J.F. Lovering, J.R. Hinthorne and R.L. Conrad, Direct $^{207}Pb/^{206}Pb$ dating by ion microprobe of uranium-thorium-rich phases in Allende calcium-aluminium-rich clasts (CARC's) (abstract), Lunar Sci. VII (1976) 504–506.